An Intelligent Detection Method for Conveyor Belt Deviation State Based on Machine Vision

Litao Sun*[iD], Xiaoxia Sun[iD]

International College, Krirk University, Bangkok 10220, Thailand

Corresponding Author Email: LT-SUN@hotmail.com

ABSTRACT

To address the shortcomings of existing conveyor belt deviation detection methods, such as poor fault location accuracy, a low automation level and low reliability, a method that utilizes machine vision technology to detect belt deviations in belt conveyors is proposed. This method involves preprocessing operations on captured video images, including Region of Interest (ROI) extraction, grayscale processing, and noise reduction, thereby eliminating image noise and interference. To address the edge blurring due to Gaussian filtering and threshold setting issues in Canny detection, an enhanced edge detection technique using a guided filter and the Otsu method modifies the traditional Canny operator is introduced. Subsequent application of Hough Transform and least squares fitting processes delineate the edges of the conveyor belt and its rollers during operation. Utilizing the detected edges of the conveyor belt and rollers as references, a dual-baseline positioning method is for the first time proposed to quantify the deviation degree, facilitating the identification of deviation faults. After detection with the improved Canny algorithm, clearer contour binary images with fewer noise and impurities were obtained. Experiments conducted on images from various deviation scenarios yielded an average detection accuracy of 95.4% and a detection speed of 26 frames per second (FPS). This approach not only enhances the detection speed and accuracy but also reduces the frequency of conveyor belt failures and improves the operational efficiency of belt conveyors.

1. INTRODUCTION

As China's economy rapidly develops, the demand for energy continues to increase. However, under the goals of peaking carbon emissions and achieving carbon neutrality, constructing a comprehensive multi-energy supply system and realizing the sustainable development and green transformation of energy have become the current crucial directions in energy development [1, 2]. China has rich coal reserves, currently ranking among the world's top in terms of coal storage and annual coal production [3, 4]. As coal remains a major source of energy in China, it is essential to develop intelligent coal machinery equipment, enhance safety management in coal production, and improve mining technology levels [5]. Gradually achieving automated and intelligent mining and the green, clean, and efficient utilization of coal resources reduces the negative environmental impacts during the mining, production, and use of coal, ensuring the healthy development of the coal mining industry [6, 7].

In the coal production process, mining belt conveyors primarily transport large quantities of coal from the mine bottom to the surface, forming an integral part of the coal mining and utilization process. The safe and stable operation of these conveyors directly affects the safety and efficiency of coal production [8]. Additionally, compared to road and rail transportation, belt conveyor systems have the advantages of large transport capacity, long transport distances, low freight

rates, high efficiency, high automation levels, continuity, and convenient loading and unloading, and are widely used in underground and open-pit coal mines [9, 10]. Conveyor belt is the most expensive part of any belt conveyor. It is responsible for 40% to 60% of the conveyor's total price [11]. Belt conveyors often operate under harsh conditions for long periods at high loads and intensities, frequently experiencing various faults [12]. Studies have shown that about 70%-80% of accidents involving belt conveyors are due to belt deviations [13]. When deviation occurs, a significant amount of coal falls from the side of the conveyor belt, severely impacting production efficiency and even threatening the safety of miners on the production line [14].

Belt deviation refers to the gradual deviation of the conveyor belt's center position from the centerline of the conveyor frame, resulting in one side widening and the other narrowing, breaking the normally symmetrical and equal-width state of the belt [15]. Such faults can cause uneven belt tension, leading to wear and deformation, spillage of materials, or the belt twisting, significantly increasing operational resistance, potentially burning out motors, causing the conveyor belt to slip, and thereby leading to even more severe accidents such as fires [16]. Therefore, monitoring the state of conveyor belt deviation is equally important for ensuring safe production, and various deviation fault monitoring methods have been proposed and applied ever since.

Traditional fault detection devices for belt conveyors

mostly rely on structural changes or physical and chemical changes to complete detection tasks. However, these devices tend to fail over long periods in harsh underground environments, reducing their reliability [17]. Current domestic and international fault detection systems for underground coal mine belt conveyors still face issues such as single functionality, poor fault localization and analysis accuracy, low automation levels, and low reliability. Moreover, the systems developed so far are generally costly and not easy to maintain [18]. Therefore, how to quickly and reliably detect and warn of failures during the operation of mining belt conveyors is an urgent problem in the safe production of coal energy.

To overcome the existing problems in fault detection technology for underground coal mine belt conveyors, this paper proposes an intelligent detection method for conveyor belt deviation faults based on machine vision. By improving the machine vision edge detection algorithm, edge images with clearer outlines and less noise and impurities are obtained, and through the conveyor belt deviation mathematical model, rapid and accurate detection of deviation faults is achieved, and enhancing the reliability of underground belt conveyor monitoring systems, effectively preventing fault omissions due to the failure of traditional detection devices.

2. LITERATURE REVIEW

2.1 Detection of conveyor belt deviation

Many experts and scholars have researched the detection of conveyor belt deviation and have proposed numerous solutions aimed at minimizing the frequency of deviation occurrences and reducing failures in belt conveyors. Existing methods for detecting conveyor belt deviation primarily include contact and non-contact methods.

Contact detection methods for conveyor belt deviation primarily utilize mechanical action deviation sensors. When the conveyor belt touches the sensor, it triggers a deviation travel switch and a knob, emitting an alarm signal. If the conveyor belt continues to deviate, a second-level knob is triggered, which then activates an emergency stop button. While this detection device is convenient to use, the sensors are significantly affected by environmental factors and often fail due to rust [19]; another method involves identifying conveyor belt deviation by measuring the deflection angle of the vertical rollers driven by the misaligned belt, using this deflection angle to detect and categorize deviation with pre-warning [20]. This mechanical structure-based pre-warning method for belt deviation is highly stable, but it cannot monitor the deviation status and trends online, and the communication between devices is complex, requiring extensive installation, deployment, and high maintenance costs.

The limitations of contact detection methods are poor reliability and accuracy. In high-speed operations, friction between the conveyor belt edge and the guide rod can cause wear and deformation of the belt and damage to sensors, often leading to false alarms or even shutdowns. Additionally, these methods have poor sensitivity, and cannot estimate the degree of deviation, thus not effectively meeting practical production needs.

Non-contact detection devices generally utilize technologies such as high-definition cameras and photoelectric sensors, combined with microcontrollers, PLCs,

and virtual machines, to form conveyor belt deviation detection and monitoring systems, but these are somewhat limited by the site environment [21]. One non-contact method uses photoelectric sensors to detect the operational status of the conveyor belt. This detection method is quite effective for ordinary deviation detection and correction, but it struggles with diagnosing faults like serpentine deviation or twisted belts [18]. Chamorro et al. [22] proposed the fusion of sensor monitoring systems and developed an algorithm for analyzing sensor data to monitor the health of conveyor systems, enabling monitoring of belt speed, belt load, and belt misalignment. However, long-term test runs are required to ensure system reliability; Stachowiak et al. [23] introduced a biomimetic inspection robot system that also relies on image processing to extract conveyor belt edge information, which has been preliminarily applied in mines.

2.2 Machine vision image detection

Machine vision image detection refers to the use of computer vision algorithms and models to detect the presence and location of specific objects, items, or patterns in images. It is a technique that utilizes artificial intelligence to transform specific image information into data that can be understood and interpreted by computers. The main steps include image acquisition, image preprocessing, feature information extraction, object detection, classification, and recognition. Machine vision image detection technology is widely used in many fields, including autonomous driving, security monitoring, medical image analysis, and industrial quality inspection [21].

Machine vision image processing is also extensively applied in the field of conveyor belt deviation monitoring, with numerous scholars conducting extensive research using machine vision image inspection technology. For instance, Wang et al. [24] proposed a method that utilizes line detection to identify the edges of a conveyor belt and measures the deviation distance to assess the extent of the belt's deviation. Zeng et al. [18] introduced a deep learning approach based on a multi-scale feature fusion network, which has been experimentally proven to be more effective than FCN and other segmentation models and the classical Canny edge detection algorithm in detecting the edges of conveyor belts. Wang et al. [25] combined the Canny operator with Hough line transformation to extract the edges of the conveyor belt, and by using morphological processing and connected component analysis, they determined the position of the conveyor belt and assessed whether deviation had occurred. Zhang et al. [26] based on Canny detection and Hough transformation, proposed an image processing mode that uses a laser projection line as a reference, also achieving monitoring of conveyor belt deviation faults. Wang et al. [21] considered the impact of dust and other factors in harsh environments, used wavelet transform to denoise and enhance coal mine conveyor belt images, employed the OpenCV vision library for image preprocessing and conveyor belt edge extraction, and designed a three-level correction mechanism involving "adjustable idler—passive drum—motor." Liu et al. [19] processed conveyor belt images captured by industrial cameras mounted on inspection robots, used Hough transformation to extract the belt edges, employed template matching to obtain information on the outer edge of the rollers, and by comparing the two, they assessed the degree of deviation, accomplishing deviation detection at any position of the segment belt conveyor.

3. MATHEMATICAL MODEL AND RESEARCH METHOD

The principle of conveyor belt deviation detection based on machine vision image processing technology proposed in this paper is as follows: Data collection is conducted through a camera located directly above the conveyor belt, capturing real-time video and transmitting the data to an edge computer for deviation detection, as shown in Figure 1. The decoded video undergoes image capture every 5 seconds. Firstly, the collected data undergo image preprocessing, including extraction of the ROI, grayscale transformation, noise processing, and histogram equalization. Then, enhanced Canny algorithm is used for edge feature extraction, and morphological filtering methods are applied to handle interference signals and false edges. Finally, through Hough transform and least squares fitting, the edges of the conveyor belt and rollers during operation are identified. Using the detected edges of the conveyor belt and rollers as a reference, a dual-baseline positioning method is designed, establishing a mathematical model for conveyor belt deviation, calculating the extent of deviation, and realizing the identification of conveyor belt deviation faults.
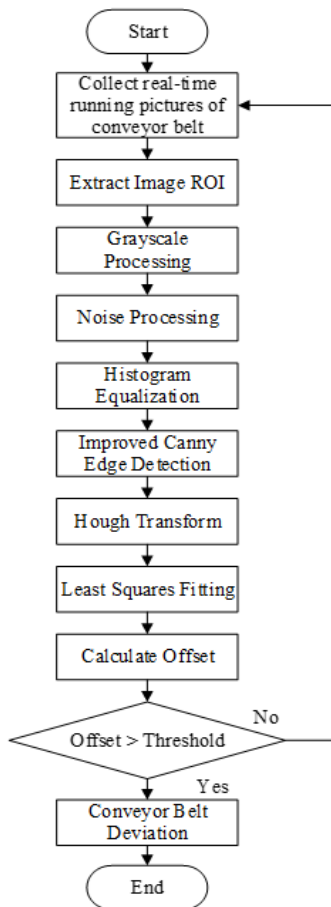

Figure 1. Flowchart of conveyor belt deviation detection

3.1 Image processing

Image preprocessing includes extracting the image ROI, grayscale transformation, noise processing, and histogram equalization. When the camera is installed directly above the conveyor belt, facing the direction of material transportation on the belt, the belt area usually occupies more than 70% of

the entire image. Therefore, the ROI is taken as 35% of the image width from the center point to both left and right, and from the top to the bottom boundary of the image. Grayscale transformation involves converting the original RGB image into a grayscale image to increase the efficiency of algorithm processing. Unprocessed grayscale images often contain noise points, which significantly affect subsequent edge detection, thus necessitating filtering operations to eliminate these noise points. After noise processing, the histogram equalization algorithm is used to stretch the image contrast, enhancing the image's dynamic range, making the black and white boundaries more prominent, and facilitating the subsequent edge detection algorithm.

(1) Grayscale processing

Grayscale processing refers to the process of converting a color image into a grayscale image. The purpose of using a grayscale image is to simplify the matrix, reduce the information channels of the image to be processed, and increase computational speed. In this study, the weighted average method is used for image grayscale processing, hence each pixel's grayscale value is the weighted average of the red, green, and blue color channels. The calculation expression is as shown in Eq. (1):

$$Gray(x, y) = 0.299 * R(x, y) + 0.587 * G(x, y) + 0.114 * B(x, y) \tag{1}$$

where, Gray(x,y) represents the pixel value of the grayscale image, and R(x,y), G(x,y), and B(x,y) respectively represent the pixel values of the red, green, and blue color channels at the (x,y) coordinates in the original image. The coefficients 0.299, 0.587, and 0.114 are standard weights used in the formula for converting color images to grayscale images.

(2) Noise processing

Considering factors such as coal dust pollution, possible camera shaking, and dim underground lighting that can reduce the clarity of the captured video images, it is necessary to filter out noise from the video images. The Wiener filter, which has the advantages of low computational load, good image restoration effects, noise suppression, and prevention of noise amplification, achieves a good balance between image clarity and noise suppression. The calculation expression is shown in Eq. (2):

$$e^2 = minE\left[\left|f(x, y) - \hat{f}(x, y)\right|^2\right] \tag{2}$$

where, e^2 represents the mean squared error between the original image and the Wiener filtered image, E is the expected value of the parameter, $f(x,y)$ is the original image, and $\hat{f}(x, y)$ is the Wiener filtered image.

(3) Histogram equalization

Histogram equalization redistributes the grayscale values in the original image, making the differences between grayscale levels more apparent, thus achieving enhanced contrast. After image filtering, using histogram equalization to stretch the image contrast enhances the image's dynamic range, making the black and white boundaries more distinct, and improving the detection effectiveness of the edge detection algorithm. The image is composed of many pixels, so the mapping method for image histogram equalization is:

$$S_k = \sum_{j=0}^{k} \frac{n_j}{n} \ (k = 0,1,2,\cdots,L-1) \tag{3}$$

where, S_k is the value after cumulative distribution of the

current gray level, n is the sum of pixels, n_j is the number of pixels in the current gray level, and L is the total number of gray levels.

3.2 Conveyor belt positioning algorithm

3.2.1 Edge detection

In the images, most important information is present at the edges, which are the boundaries where there is a sharp change in grayscale. The Canny algorithm is a commonly used edge detection algorithm, which involves the following four steps: (1) Gaussian filtering of the image; (2) calculation of gradient magnitude and direction; (3) non-maximum suppression; (4) double threshold filtering and edge linking.

However, during the detection process, Gaussian filtering uses the weighted average of pixel neighborhoods to replace the pixel values at the detection points, reducing the grayscale differences at the boundaries and causing blurred edges. The manual setting of dual thresholds cannot adapt to changes in the environment, leading to extracted edges that are discontinuous and incomplete. To avoid these issues with Canny edge detection, this paper uses an improved Canny edge detection algorithm based on guided filtering and the maximum inter-class variance method (Otsu method) for detecting the edges of conveyor belts and rollers.

The image gradient calculation in the Canny algorithm detection process is very sensitive to noise signals. This paper uses guided filtering technology to remove noise interference signals. The principle is that a point on the image and its neighboring parts can form a linear model, so the overall image filtering function can be represented by multiple local linear models. The grayscale average of a point's pixel is taken from the average of all local linear models that include that point, thus achieving filtering in any direction. During the guided filtering process, the filtered grayscale value of a pixel in the image is given by Eq. (4).

$$q_i = \Sigma_j W_{i,j}(I)p_j \qquad (4)$$

where i and j represent pixel points; q_i is the pixel value of the output image; I is the guide image; p is the input image; $W_{i,j}$ is the kernel function between the guide image I and the input image p.

Define ω_k as the filtering window for pixel k, then the local linear model between the output image q and the guide image I can be expressed using Eq. (5).

$$q_i = a_k I_i + b_k , \forall i \in \omega_k \qquad (5)$$

Taking the gradient on both sides of Eq. (4), we can get Eq. (6):

$$\nabla q = a\nabla I \qquad (6)$$

Further minimization of the window ω_k results in the loss function within the filtering window as shown in Eq. (7).

$$E(a_k, b_k) = \Sigma_{i \in \omega_k}((a_k I_i + b_k - p_i)^2 + \varepsilon a_k^2) \qquad (7)$$

From this, the values of a and b are calculated, as shown in Eqs. (8) and (9), and thus the output image q can be obtained.

$$a_k = \frac{\frac{1}{|\omega|}\Sigma_{i \in \omega_k}I_i p_i - \mu_k \overline{p_k}}{\sigma_k^2 + \varepsilon} \qquad (8)$$

$$b_k = \bar{p}_k - a_k \mu_k \qquad (9)$$

where, ε is the smoothing factor for a_k, $\bar{p}_k = \frac{1}{|w|}\Sigma_{i \in \omega_k}p_i$ is the average of p in ω_k, $|\omega|$ is the number of pixels in the window, μ_k and σ_k^2 are the mean and variance of the pixel intensities within the window. Using the guided filtering method for filtering the conveyor belt edge images not only effectively eliminates high-frequency parts of the image but also retains the grayscale gradients of the edges, maintaining good conveyor belt edge features, and laying a solid foundation for subsequent edge detection.

To avoid the problems of manually setting high and low threshold parameters in the original algorithm, which cannot adapt to environmental changes, this paper uses the Otsu algorithm to automatically determine the optimal threshold by using the image's grayscale histogram to divide the image pixels into two categories: background and target. If the inter-class variance between the background and target is larger, it indicates a greater difference between the background and target in the image, thus a more accurate classification. When the background and target classification is incorrect, it leads to a smaller inter-class variance. Therefore, the optimal threshold is when the inter-class variance is maximized. Assuming the segmentation threshold between the target and background is T, the proportion of target pixels in the image is ω_0, and the average grayscale is μ_0; the proportion of background pixels is ω_1, and the average grayscale is μ_1. The total average grayscale μ, and the inter-class variance g between the target and background can be expressed using Eqs. (10) and (11), with a constraint relationship as shown in Eq. (12).

$$\mu = \omega_0\mu_0 + \omega_1\mu_1 \qquad (10)$$

$$g = \omega_0(\mu_0 - \mu)^2 + \omega_1(\mu_1 - \mu)^2 \qquad (11)$$

$$\omega_0 + \omega_1 = 1 \qquad (12)$$

Substituting Eq. (12) into Eq. (11) yields:

$$g = \omega_0\omega_1(\mu_0 - \mu_1)^2 \qquad (13)$$

As shown in Eq. (13), when the inter-class variance g is maximized, the difference in grayscale values between the foreground and background in the image is maximized, and thus the threshold $T = g_{max}$. Therefore, the high threshold T_h for the Canny operator is set to T, and based on experience, the low threshold is typically set to 0.3 to 0.5 times the high threshold. In this paper, the low threshold T_l is chosen as $0.4 * T_h$.

The steps of the improved Canny edge detection algorithm are as follows: First, guided filtering is used to smooth and filter the grayscale image of the original image, reducing noise interference and preserving edge information. Second, the Sobel operator is used to calculate the gradient. Third, non-maximum suppression is applied to remove non-maximum points in the positive and negative gradient directions, retaining maximum gradient points. Fourth, the Otsu algorithm with a suppression factor is used to adaptively select the threshold T, and this value is set as the high threshold $T_h = T$ for the Canny operator, with the low threshold $T_l = 0.4 * T_h$. The final step involves using the double threshold method to detect, retaining strong edges and weak edges connected to strong edges, filtering out other interferences.

3.2.2 Line extraction

The Hough transform is widely used in line detection due to its robustness and strong noise resistance. Its principle involves a transformation of parameters between different spaces. Specifically, a line in the Cartesian coordinate system can be mapped to a point in the Hough parameter space, forming a peak point. This transforms the problem of line detection in the Cartesian coordinate system into a problem of peak statistics in the Hough parameter space, allowing for detection even if the spatial shape is partially obscured or distorted in the image. As lines parallel to the y-axis in the Cartesian coordinate system do not exist or have an infinite slope, it is necessary to transform the line representation from Cartesian coordinates to polar coordinates before mapping to the Hough space, as shown in Figure 2.

In the Hough transform, the representation of lines in polar coordinates is used, as shown in Eq. (14).

$$\rho = x\cos\theta + y\sin\theta \tag{14}$$

where, ρ is the distance from the origin to the line, and θ is the angle between the x-axis and the line.

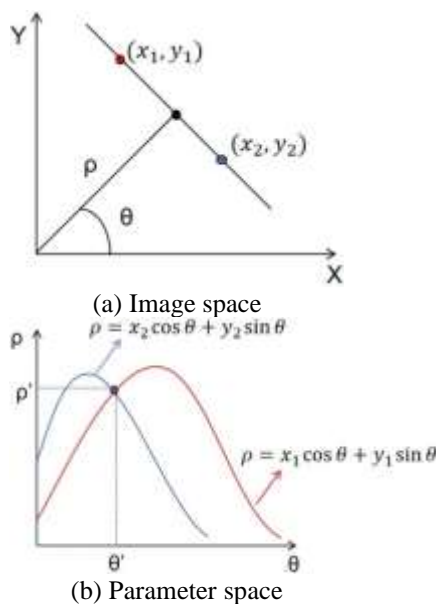(a) Image space

(b) Parameter space

Figure 2. Schematic of the Hough transform dual relationship

3.2.3 Least squares fitting

Least squares fitting is a commonly used linear fitting method in engineering that aims to find the best fit parameters by minimizing the sum of the squares of the residuals, thereby ensuring that the model's predicted values closely match the observed data. Its advantage lies in providing a simple yet powerful method to estimate model parameters, allowing the model to adapt to the observed data. This paper utilizes the least squares method to achieve linear fitting of line segments near the conveyor belt edge, thereby correcting the edges of the rollers and the conveyor belt.

3.3 Method for calculating deviation

Under normal conditions, the center position of the conveyor belt coincides with the centerline of the conveyor frame. As the distribution of transported materials changes or due to other variable factors, the position of the conveyor belt may shift. However, the relative positions of the rollers on both sides of the conveyor will not change, and the outer edges of the rollers on both sides of the belt conveyor will form two straight lines. The midline of these two lines is considered the centerline of the frame. Therefore, this paper proposes a method for determining conveyor belt deviation using the straight lines formed by the edges of the rollers of the belt conveyor. The deviation of the conveyor belt is calculated by measuring the distance from the midline of the conveyor belt edges to the midline of the rollers on both sides, as shown in the schematic diagram in Figure 3.
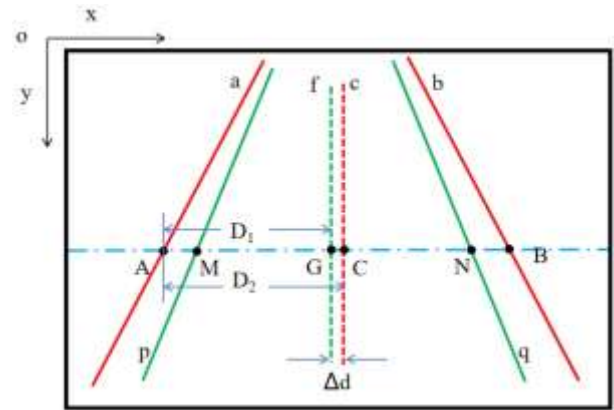

Figure 3. Schematic diagram of conveyor belt deviation judgment model

As shown in Figure 3, the coordinate system is established at the top left corner of the image, and a virtual reference line is constructed, which is the blue dashed line parallel to the x-axis. The red lines a and b on both sides of the image are the lines formed after fitting the edges of the rollers, and the green lines p and q are the straight lines formed after fitting the edges of the conveyor belt. The intersection points of the virtual reference line with lines a and b are A and B, respectively, and segment AB is the connecting line of the rollers on the left and right. The intersection points of the virtual reference line with lines p and q are M and N, respectively, and segment MN is the line on the conveyor belt, with both MN and AB parallel to the x-axis. The green dashed line f is the midline of segment MN, intersecting the virtual reference line at point G. The red dashed line c is the centerline of segment AB, intersecting the virtual reference line at point C.

Using the coordinates of each pixel, the straight lines p and q of the left and right edges of the conveyor belt can be fitted, as well as the outermost lines a and b on both sides of the rollers. Based on the midpoint $G(x_G, y_G)$ determined by points $M(x_M, y_M)$ and $N(x_N, y_N)$ on the edge of the conveyor belt, the midline f of the conveyor belt in actual operation can be obtained:

$$G(x_G, y_G) = G(\frac{x_M + x_N}{2}, \frac{y_M + y_N}{2}) \tag{15}$$

Similarly, based on the midpoint $C(x_C, y_C)$ determined by points $A(x_A, y_A)$ and $B(x_B, y_B)$ on the fitted lines of the rollers, the midline c of the left and right rollers can be determined:

$$C(x_C, y_C) = C(\frac{x_A + x_B}{2}, \frac{y_A + y_B}{2}) \tag{16}$$

When the conveyor belt is not misaligned, line f coincides

with line c. When the conveyor belt is misaligned, the distance D_2 from point A to line c is the distance from point A to point C:

$$D_2 = \sqrt{(x_C - x_A)^2 + (y_C - y_A)^2} \qquad (17)$$

The distance D_1 from point A to line f is the distance from point A to point G:

$$D_1 = \sqrt{(x_G - x_A)^2 + (y_G - y_A)^2} \qquad (18)$$

Therefore, the distance between line f and line c is:

$$\Delta d = |D_2 - D_1| \qquad (19)$$

Thus, Δd is the actual deviation distance of the conveyor belt. When the edges of the conveyor belt coincide with the external connection lines of the rollers, i.e., when line a coincides with line p, it represents the maximum value of conveyor belt deviation. At this time, the distance D_{1min} from point A to line f is at its minimum, so the maximum distance Δd_{max} between line f and line c is:

$$\Delta d_{max} = |D_2 - D_{1min}| \qquad (20)$$

Consequently, the overall offset E_s of the conveyor belt is:

$$E_s = \frac{\Delta d}{\Delta d_{max}} \times 100\% \qquad (21)$$

When $D_1 < D_2$ and the actual overall offset E_s of the conveyor belt exceeds 20%, it can be determined as deviation to the left; When $D_1 > D_2$ and E_s exceeds 20%, it can be determined as deviation to the right.

4. EXPERIMENT AND ANALYSIS

The experimental subject was a YF19072-BCR300 model conveyor at a certain mine. The video image analysis software was written in Python and deployed on a supervisory computer. Video images were captured by a Hikvision MV-CE050-31GM model industrial area array CMOS camera installed above the conveyor. The video stream was processed frame by frame to obtain test images, including images of the conveyor belt in normal condition and deviated conveyor belt images.

First, the test image is subjected to image preprocessing. As shown in Figure 4(b), after grayscale processing of the original color image, the image contains only one color, with its pixel values changing from three channels to a single channel, which is beneficial for subsequent image processing to improve image quality and processing speed.

After removing blurred Gaussian noise with Wiener filtering, the clarity of the grayscale image was significantly improved, and overly bright noise points were filtered out, as shown in Figure 5.

Figures 6(a) and (b) show a comparison between the results of the traditional Canny algorithm and the images after the improved Canny edge detection, where white represents the object's edge contour, and black represents the background. In the image processed by the traditional Canny algorithm, the bulk materials transported on the conveyor belt have a lot of fine edge noise, and the edges on both sides of the conveyor belt are blurred and have few straight-line features. After detection with the improved Canny algorithm, the conveyor

belt located in the middle of the image has almost no noise, and the left and right edges of the conveyor belt are mostly preserved. Thence clearer contour binary images with fewer noise and impurities were obtained. The straight lines of the left and right edges of the conveyor belt and the rollers' contours are clearly visible in the images.
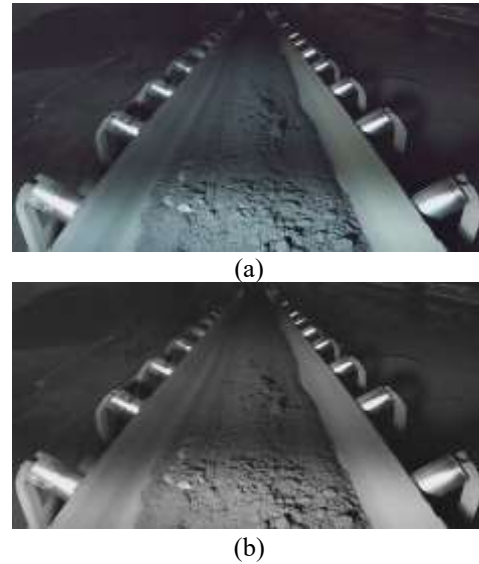

(a)

(b)

Figure 4. Image grayscale processing: (a) Original image; (b) Grayscale processed image

Figure 5. Image after wiener filtering
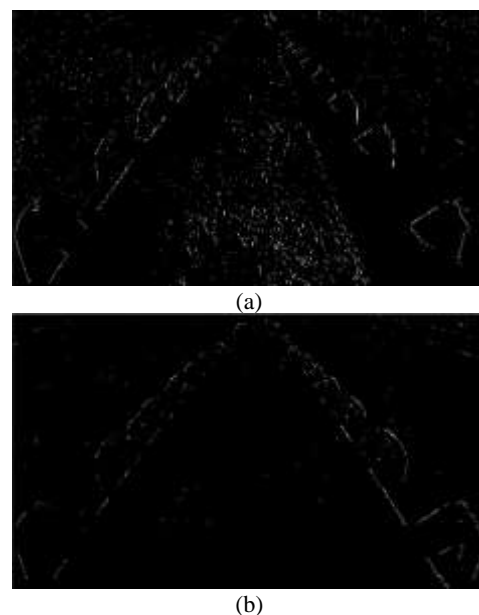

(a)

(b)

Figure 6. Conveyor belt edge line feature extraction: (a) Traditional canny algorithm result; (b) Image after improved canny edge detection

Hough Transform was used to detect multiple groups of lines that might represent the edges of the conveyor belt and rollers. Detected lines were divided into two groups based on their slope: lines with a positive slope were grouped as the left line group, and those with a negative slope were grouped as the right line group. Subsequently, the average slope for the left and right line groups was calculated independently. Lines significantly deviating from the average slope on the left were removed from the left line group, and similarly, lines in the right group significantly different from the average slope on the right were also removed. Finally, the remaining lines in the left and right groups were fitted to the left and right edges respectively using least squares method, as shown by the green lines in Figure 7 for the conveyor belt edges, and the red lines for the outermost edges of the rollers. Additionally, using the method described in Section 3 for detecting the amount of deviation of the conveyor belt, the offset between the conveyor belt edges and the reference line of the rollers was calculated. If the offset exceeds a predefined threshold, it is identified as conveyor belt deviation. If $D_1 < D_2$, the conveyor belt is determined to be misaligned to the left; if $D_1 > D_2$, the conveyor belt is determined to be misaligned to the right.
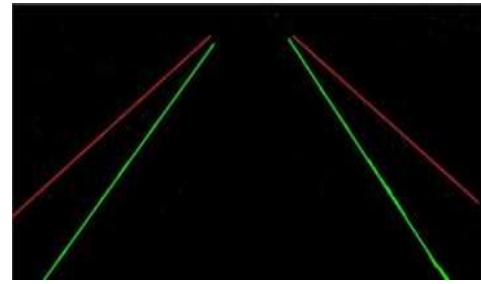

Figure 7. Image after Hough transform and least squares fitting

From the collected 300 test images, 100 images each of no deviation, left deviation, and right deviation were selected for testing using the methods described above. The test results are presented in Table 1.

Table 1. Results of conveyor belt deviation detection

Conveyor Belt Operational State	Number of Images				Missed Detection Rate (%)	Accuracy (%)	Average Processing Time (ms)
	Sample Images	Identified Images	Successfully Detected Images	Incorrectly Detected Images			
Left deviation	100	100	96	4	0	96.0	37.4
Normal	100	100	97	3	0	97.0	35.2
Right deviation	100	100	93	7	0	93.0	38.3

As shown in Table 1, under normal conditions, the miss detection rate is 0, and there are 3 images with false detected, giving an accuracy rate of 97.0%; under deviation conditions, the miss detection rate is 0, with 11 images showing false detected, resulting in an average accuracy rate of 94.5%. Therefore, the combined average detection accuracy for all samples is 95.4%.

On one hand, some images captured during the experiment were close to the deviation threshold of the conveyor belt, making it difficult for the human eye to discern whether there was deviation, leading to incorrect classification of the deviation status in the samples. On the other hand, during the edge detection and line extraction processes, there were some discrepancies between the detected belt edges and the actual belt edges, and some sample pictures collected in a dark and dusty environment have limited light intensity and low image clarity, causing slight fluctuations in accuracy. However, since the belt conveyor operation manual allows for deviation within a reasonable range during operation, this does not affect the actual deviation detection results.

Additionally, as shown in Table 1, the average processing time per photo for the conveyor belt deviation detection method is less than 38.3 ms, and the computer can complete frame detection in this time, processing 26 frames per second (FPS), which means the detection speed reaches 26 FPS. Thus, the conveyor belt deviation detection method proposed in this study can to some extent meet the requirements for real-time deviation fault status detection.

5. CONCLUSIONS

In response to the needs for the development of intelligent mining equipment, this paper proposes an intelligent detection method for conveyor belt deviation faults, achieving relatively rapid and accurate detection of conveyor belt deviation conditions. This study replaces traditional contact deviation sensors with machine vision image detection, reducing the need for maintenance personnel and enhancing the level of automation in the detection system, which helps to promote the development of belt conveyor systems. The contents of this study are summarized as follows:

(1) This paper performed a series of preprocessing operations on the collected video images, including ROI extraction, grayscale processing, and noise removal, to improve computational efficiency and effectively eliminate noise and false edges. An improved edge detection method based on guided filtering and the Otsu method was used, followed by Hough Transform and least squares fitting to obtain the edges of the conveyor belt and rollers during operation.

(2) A dual baseline positioning method was proposed, using the detected edges of the conveyor belt and rollers as references to establish a mathematical model for detecting the deviation state of the conveyor belt. This model calculated the degree of deviation and is used to identify the deviation fault state of the conveyor belt.

(3) An intelligent detection method for conveyor belt deviation state based on machine vision technology was designed and tested. In experiments, 300 images of conveyor belt shifts under different operational conditions were detected and evaluated, achieving an average detection accuracy of 95.4% and a detection speed of 26 FPS, thus enabling fast and accurate detection of deviation fault states. The detection error in this study was relatively large in insufficient lighting and dusty environments. In the follow-up research, it is aimed to solve this problem and propose an effective method to correct the deviation to ensure the stable and safe operation of the belt conveyor.

REFERENCES

[1] Hoang, A.T., Pham, V.V., Nguyen, X.P. (2021). Integrating renewable sources into energy system for smart city as a sagacious strategy towards clean and sustainable process. Journal of Cleaner Production, 305: 127161. https://doi.org/10.1016/j.jclepro.2021.127161

[2] Liu, Z., Deng, Z., He, G., Wang, H.L., Zhang, X., Lin, J., Qi, Y., Liang, X. (2022). Challenges and opportunities for carbon neutrality in China. Nature Reviews Earth & Environment, 3: 141-155. https://doi.org/10.1038/s43017-021-00244-x

[3] Zhang, W.R., Ren, M.J., Kang, J.J., Zhou, Y.O., Yuan, J.H. (2022). Estimating stranded coal assets in China's power sector. Utilities Policy, 75: 101352. https://doi.org/10.1016/j.jup.2022.101352

[4] Zhang, X.T., Ning, Y.C., Lu, C.J. (2022). Evaluation of coal supply and demand security in China and associated obstacle factors. Sustainability, 14(17): 10605. https://doi.org/10.3390/su141710605

[5] Li, Q.S. (2021). The view of technological innovation in coal industry under the vision of carbon neutralization. International Journal of Coal Science & Technology, 8: 1197-1207. https://doi.org/10.1007/s40789-021-00458-w

[6] Wang, G.F., Xu, Y.X., Ren, H.W. (2019). Intelligent and ecological coal mining as well as clean utilization technology in China: Review and prospects. International Journal of Mining Science and Technology, 29(2): 161-169. https://doi.org/10.1016/j.ijmst.2018.06.005

[7] Wang, Y., Lei, Y.X., Wang, S.Y. (2020). Green mining efficiency and improvement countermeasures for China's coal mining industry. Frontiers in Energy Research, 8: 18. https://doi.org/10.3389/fenrg.2020.00018

[8] Pan, R.K., Gao, R.X., Chao, J.K., Jia, H.L. (2023). Thermal characteristics analysis of conveyor belt during ignition. Combustion Science and Technology, 1-19. https://doi.org/10.1080/00102202.2023.2258550

[9] He, D.J., Pang, Y.S., Lodewijks, G., Liu, X.W. (2018). Healthy speed control of belt conveyors on conveying bulk materials. Powder Technology, 327: 408-419. https://doi.org/10.1016/j.powtec.2018.01.002

[10] Kawalec, W., Król, R., Suchorab, N. (2020). Regenerative belt conveyor versus haul truck-based transport: Polish open-pit mines facing sustainable development challenges. Sustainability, 12(21): 9215. https://doi.org/10.3390/su12219215

[11] Błażej, R., Jurdziak, L., Kozłowski, T., Kirjanów, A. (2018). The use of magnetic sensors in monitoring the condition of the core in steel cord conveyor belts-Tests of the measuring probe and the design of the DiagBelt system. Measurement, 123: 48-53. https://doi.org/10.1016/j.measurement.2018.03.051

[12] Wang, B.J., Dou, D.Y., Shen, N. (2023). An intelligent belt wear fault diagnosis method based on deep learning. International Journal of Coal Preparation and Utilization, 43(4): 708-725. https://doi.org/10.1080/19392699.2022.2072306

[13] Andrejiova, M., Grincova, A., Marasova, D. (2020). Monitoring dynamic loading of conveyer belts by measuring local peak impact forces. Measurement, 158: 107690. https://doi.org/10.1016/j.measurement.2020.107690

[14] Zhang, M.C., Shi, H., Zhang, Y., Yu, Y., Zhou, M.S. (2021). Deep learning-based damage detection of mining conveyor belt. Measurement, 175: 109130. https://doi.org/10.1016/j.measurement.2021.109130

[15] Sun, X.X., Wang, Y.Q., Meng, W.J. (2022). Evaluation system of curved conveyor belt deviation state based on the ARIMA–LSTM combined prediction model. Machines, 10(11): 1042. https://doi.org/10.3390/machines10111042

[16] Bortnowski, P., Kawalec, W., Król, R., Ozdoba, M. (2022). Types and causes of damage to the conveyor belt-review, classification and mutual relations. Engineering Failure Analysis, 140: 106520. https://doi.org/10.1016/j.engfailanal.2022.106520

[17] Alharbi, F., Luo, S.H., Zhang, H.Y., Shaukat, K., Yang, G., Wheeler, C.A., Chen, Z.Y. (2023). A brief review of acoustic and vibration signal-based fault detection for belt conveyor idlers using machine learning models. Sensors, 23(4): 1902. https://doi.org/10.3390/s23041902

[18] Zeng, C., Zheng, J.F., Li, J.Y. (2019). Real-time conveyor belt deviation detection algorithm based on multi-scale feature fusion network. Algorithms, 12(10): 205. https://doi.org/10.3390/a12100205

[19] Liu, Y., Miao, C.Y., Li, X.G., Xu, G.W. (2021). Research on deviation detection of belt conveyor based on inspection robot and deep learning. Complexity. https://doi.org/10.1155/2021/3734560

[20] Wang, Z., Li, J.C., Yang, X.H., Wang, H.L., Wang, L. (2023). Automatic detection method of conveyor belt deviation based on DeepLabv3+. In International Conference on Internet of Things and Machine Learning (IoTML 2022).

[21] Wang, T.H., Dong, Z., Liu, J.Q. (2021). Research of mine conveyor belt deviation detection system based on machine vision. Journal of Mining Science, 57: 703-712. https://doi.org/10.1134/S1062739121040190

[22] Chamorro, J., Vallejo, L., Maynard, C., Guevara, S., Solorio, J. A., Soto, N., Singh, K.V., Bhate, U., Kumar G.V.V.,R., Garcia, J., Newell, B. (2022). Health monitoring of a conveyor belt system using machine vision and real-time sensor data. CIRP Journal of Manufacturing Science and Technology, 38: 38-50. https://doi.org/10.1016/j.cirpj.2022.03.013

[23] Stachowiak, M., Koperska, W., Stefaniak, P., Skoczylas, A., Anufriiev, S. (2021). Procedures of detecting damage to a conveyor belt with use of an inspection legged robot for deep mine infrastructure. Minerals, 11(10): 1040. https://doi.org/10.3390/min11101040

[24] Wang, M., Shen, K.J., Tai, C.W., Zhang, Q.F., Yang, Z.Y., Guo, C.B. (2023). Research on fault diagnosis system for belt conveyor based on internet of things and the LightGBM model. PLOS ONE, 18(3): e0277352. https://doi.org/10.1371/journal.pone.0277352

[25] Wang, J.B., Liu, Q., Dai, M.T. (2019). Belt vision localization algorithm based on machine vision and belt conveyor deviation detection. In 2019 34rd Youth Academic Annual Conference of Chinese Association of Automation (YAC), Jinzhou, China, pp. 269-273. https://doi.org/10.1109/YAC.2019.8787667

[26] Zhang, M.C., Shi, H., Yu, Y., Zhou, M.S. (2020). A computer vision based conveyor deviation detection system. Applied Sciences, 10(7): 2402. https://doi.org/10.3390/app10072402